Biochimica et Biophysica Acta 1818 (2012) 146–153

Contents lists available at ScienceDirect

Biochimica et Biophysica Acta

journal homepage: www.elsevier.com/locate/bbamem

Probing ground and excited states of phospholamban in model and native lipid membranes by magic angle spinning NMR spectroscopy☆

Martin Gustavsson [a], Nathaniel J. Traaseth [a,1], Gianluigi Veglia [a,b,*]

[a] Department of Biochemistry, Molecular Biology, and Biophysics, University of Minnesota, Minneapolis, MN 55455, USA
[b] Department of Chemistry, University of Minnesota, Minneapolis, MN 55455, USA

ARTICLE INFO

Article history:
Received 4 June 2011
Received in revised form 27 July 2011
Accepted 28 July 2011
Available online 3 August 2011

Keywords:
Membrane protein
NMR
Phospholamban
Excited states
Lipid bilayers
Magic angle spinning

ABSTRACT

In this paper, we analyzed the ground and excited states of phospholamban (PLN), a membrane protein that regulates sarcoplasmic reticulum calcium ATPase (SERCA), in different membrane mimetic environments. Previously, we proposed that the conformational equilibria of PLN are central to SERCA regulation. Here, we show that these equilibria detected in micelles and bicelles are also present in native sarcoplasmic reticulum lipid membranes as probed by MAS solid-state NMR. Importantly, we found that the kinetics of conformational exchange and the extent of ground and excited states in detergent micelles and lipid bilayers are different, revealing a possible role of the membrane composition on the allosteric regulation of SERCA. Since the extent of excited states is directly correlated to SERCA inhibition, these findings open up the exciting possibility that calcium transport in the heart can be controlled by the lipid bilayer composition. This article is part of a Special Issue entitled: Membrane protein structure and function.

1. Introduction

Membrane proteins exist as ensembles (Boltzmann distribution) of ground and excited states. These states are accessible by small scale atomic fluctuations around the average structure or large scale reorganizations of entire domains. In addition to intrinsic thermal fluctuations, the membrane protein folding energy landscape is shaped by the interactions with the lipid membrane, which have been hypothesized to modulate protein function through allosteric interactions [1]. In the past years, the need to obtain high-resolution membrane protein structures for structural genomics initiatives drove researchers toward high-quality views of average conformations or crystallographic snapshots of membrane proteins in non-native detergent micellar environments. The latter effectively relegated the analysis of conformational fluctuations and protein–lipid interactions to secondary roles. While the structures have given us vivid views of static membrane proteins, our knowledge on how these biological macromolecules transmit the regulatory effects through the membrane at the atomic level is still primordial. It is clear that a complete description of membrane protein function must include: structure, the motions (conformational dynamics), and their interactions with lipid membranes. Magic angle spinning (MAS) NMR [2–12] and oriented solid-state (OSS) NMR [13–18] have evolved as powerful methods to study the structure and dynamics of membrane proteins in native-like lipid bilayers. While the development of these solid-state NMR techniques will be instrumental to determine the structure of large membrane proteins, their major advantage with respect to X-ray crystallography will be to describe membrane proteins as ensemble of structures, including ground and excited states.

In the past years, our group has focused attention on the small membrane protein phospholamban (PLN, 52-residue) that regulates the function of sarcoplasmic reticulum (SR) Ca^{2+}-ATPase (SERCA) in cardiac muscle [19,20]. While apparently simple in its secondary structure content, PLN has a complex dynamics when reconstituted both in micelles and synthetic lipid membranes [21–23]. In its monomeric and pentameric forms, PLN consists of a membrane spanning helix connected to an amphipathic helix (domain Ia) through a short loop [15,16,24] (Fig. 1). The membrane-spanning helix can be divided into a rigid and hydrophobic domain II and a more dynamic and hydrophilic domain Ib, which is positioned at the lipid head group/water interface and unfolds on a μs time scale [21,25]. Domain Ia of PLN is in a pre-existing conformational equilibrium that involves at least four different states and resembles the folding/unfolding proposed for amphipathic helices: detached/

Abbreviations: PLN, Phospholamban; SERCA, sarcoplasmic reticulum Ca^{2+}-ATPase; DMPC, 1,2-dimyristoyl-sn-glycero-3-phosphocholine; DHPC, 1,2-dihexanoyl-sn-glycero-3-phosphocholine; DPC, dodecylphosphocholine; DMPG, 1,2-dimyristoyl-*sn*-glycero-3-phospho-(1′-rac-glycerol); MLVs, multi-lamellar lipid vesicles

☆ This article is part of a Special Issue entitled: Membrane protein structure and function.

* Corresponding author at: Department of Biochemistry, Molecular Biology & Biophysics, University of Minnesota, 6-155 Jackson Hall, 321 Church Street SE, Minneapolis, MN 55455, USA. Tel.: +1 612 625 0758; fax: +1 612 626 7541.
E-mail address: vegli001@umn.edu (G. Veglia).
[1] Present address: Chemistry Department, New York University, New York, NY 10003, USA.

0005-2736/$ – see front matter © 2011 Elsevier B.V. All rights reserved.
doi:10.1016/j.bbamem.2011.07.040

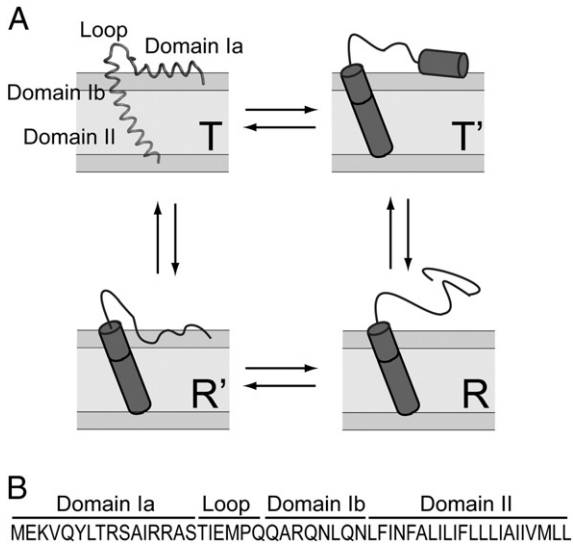

Fig. 1. Conformational equilibria and primary sequence. A.) Conformational equilibria of monomeric PLN. The T state is represented by its high resolution structure (PDB ID: 2KB7) [16]. B.) Primary sequence of AFA-PLN.

unfolded (R), absorbed/unfolded (R′), absorbed/partially folded (T′), and absorbed/fully folded (T) [26–28]. For monomeric and pentameric PLN, the R state has a small population in DPC detergent micelles and mechanically aligned lipid bilayers (<15%) [28]. Although most of the information on the high energy (excited) R, T′ and R′ states was derived from studies in detergent micelles, we found a direct relationship between the population of these excited states and PLN inhibition of SERCA, i.e., the more populated is the R state, the less inhibitory is PLN [26,29]. This structure–function correlation is being exploited to design loss-of-function PLN analogs to be used in gene therapy [30,31].

To understand how PLN's conformational equilibria are modulated by lipid membrane composition, we utilized Magic Angle Spinning (MAS) solid-state NMR in conjunction with solution NMR methods. We show that, although the relative populations of the different states can be tuned by the type and charge of lipids, a conformational equilibrium of PLN is present in all of the membrane mimicking systems analyzed, ranging from dodecylphosphocholine (DPC) micelles and 1,2-dimyristoyl-sn-glycero-3-phosphocholine/1,2-dihexanoyl-sn-glycero-3-phosphocholine (DMPC/DHPC) bicelles to native SR lipid bilayers. These results demonstrate the presence and importance of conformational fluctuations in native cellular membranes.

2. Materials and methods

2.1. Sample preparation

Synthetic lipids and natural egg PC, phosphatidylethanolamine (PE) and phosphatidic acid (PA) lipids were purchased from Avanti polar lipids (Alabaster, AL). Native SR lipids were extracted from rabbit hind leg skeletal muscle using a chloroform:methanol procedure as previously described [32]. All experiments utilized a monomeric PLN mutant with Cys36, 41, and 46 mutated to Ala, Phe, and Ala, respectively (AFA-PLN) [33]. [U-^{13}C, ^{15}N] AFA-PLN was recombinantly expressed in *E. coli* and purified according to Buck et al. [34] [EQN-^{13}C, ^{15}N; A-^{13}C] AFA-PLN was produced by a reversed labeling method, where unlabeled analogs of all other amino acids were added to the growth medium which also contained ^{13}C-glucose and $^{15}NH_4Cl$ [35]. Selectively [^{15}N, ^{13}C] labeled AFA-PLN was synthesized using [^{15}N, ^{13}C] labeled amino acids (Sigma-Aldrich, Isotec, Miamisburg, OH) on a microwave peptide synthesizer (CEM Corporation, Matthews, NC) essentially as previously described [16,33]. The exceptions were that 1% sodium dodecyl sulfate (SDS) was added during cleavage from the resin and the protein was dissolved in 10% SDS prior to HPLC purification, which utilized a 2-propanol/H_2O gradient from 10% to 90% on a C8 column. To avoid oxidation of Met50, we made a conservative substitution to norleucine in the synthetic samples. This substitution had no effect on the inhibitory effect of AFA-PLN on SERCA. The quality of the final synthetic product was assessed by mass spectrometry and solution NMR in DPC micelles. SERCA activity assays were performed as described previously [29,36] to confirm that all recombinantly and synthetically produced AFA-PLN proteins inhibited SERCA.

Isotropic bicelle samples for solution NMR were prepared by dissolving 1 mg of [U-^{13}C, ^{15}N] AFA-PLN in a 174 mg/mL solution of DHPC containing 20 mM MOPS, 100 mM NaCl, and 5% D_2O. The protein/DHPC solution was added to 21.9 mg of lyophilized DMPC lipids, and was followed by several freeze/thaw cycles to form a clear bicellar solution. The pH was adjusted to 7.0 and the 250 μL sample containing a DMPC:DHPC molar ratio (q) of 0.33 was transferred to a 5 mm Shigemi tube. Negatively charged bicelles were prepared identically with the exception that 33% of the DMPC was replaced by 1,2-dimyristoyl-*sn*-glycero-3-phospho-(1′-rac-glycerol) (DMPG).

MAS samples were prepared by dissolving 15 mg of lyophilized lipids in HPLC elution (~70% 2-propanol, ~30% H_2O) containing 1.6 mg AFA-PLN. To this solution, 20 mM MOPS (pH 7.0) and 100 mM NaCl were added based on a final volume of 2 mL. The 2-propanol was then evaporated using nitrogen gas to form AFA-PLN-containing multi-lamellar lipid vesicles (MLVs). The mixture was lyophilized, re-suspended in 2 mL of double distilled H_2O and centrifuged at 200,000 ×*g* to yield a hydrated lipid pellet, which was transferred to a 3.2 mm thin wall rotor MAS rotor. The final samples contained ~60% H_2O and had a lipid:AFA-PLN ratio of ~80:1. For paramagnetic quenching experiments, gadopentetate dimeglumine (Gd^{3+}) (Magnevist; Bayer Shering Pharma, Berlin, Germany) was added to the MAS sample and several freeze/thaw cycles were performed (final Gd^{3+} concentration was 20 mM).

2.2. NMR experiments

All NMR experiments were performed on a Varian (VNMRS) spectrometer operating at a proton frequency of 600 MHz. Solution NMR chemical shifts of AFA-PLN in isotropic bicelles were assigned using two-dimensional HNCO, HN(CO)Cα, and HNCαCβ experiments and were referenced to 2,2-dimethyl-2-silapentane-5-sulfonate (DSS). Chemical shifts in MLVs were assigned using SPC5 single quantum double quantum correlation (SQ-DQ) [40], dipolar assisted rotational resonance (DARR) [37], and refocused Insensitive Nuclei Enhanced by Polarization Transfer [38] (rINEPT) experiments acquired using a ^{1}H/^{13}C 3.2 mm BioMAS Varian probe. Pulse widths corresponding to a flip angle of π/2 were typically 5.5 μs (^{13}C, ^{15}N) and 2.5 μs (^{1}H). Proton TPPM decoupling [39] was applied at $\omega_1/(2\pi) =$ 100 kHz. SQ-DQ experiments were acquired at a spinning rate of 8 kHz, a cross-polarization (CP) time of 1 ms and spectral widths of 100 and 16 kHz in the single and double quantum dimensions, respectively. A 500 μs SPC5 element [40] was used for excitation and reconversion. DARR experiments were acquired with a 200 ms mixing time at a spinning speed of 13.3 kHz and a 1 ms cross-polarization (CP) time. 4000 points with a spectral width of 100 kHz and 30 increments with a spectral width of 13.3 kHz were acquired in the direct and indirect ^{13}C dimensions, respectively. rINEPT experiments were acquired at the same spinning rate with the same number of points and spectral width in the direct ^{13}C dimension and 30 increments with a spectral width of 3.33 kHz in the indirect ^{1}H dimension. Chemical shifts were referenced to the CH_2 signal of adamantane (40.48 ppm). Data were processed by NMRPipe [41] and analyzed with Sparky [42].

3. Results

3.1. Residue-specific assignments in lipid bilayers

Due to the lack of residue-specific resolution in [U-^{13}C, ^{15}N] MAS spectra, we opted to assign chemical shifts of AFA-PLN from synthetically labeled AFA-PLN reconstituted into egg PC/PE/PA 8/1/1 MLVs (labeling is shown in Table 1). Using a [QNE-^{13}C, ^{15}N, A-^{13}C]-labeled sample, we unambiguously assigned backbone and side chain chemical shifts for domain Ib and II from single-quantum double-quantum (SQ-DQ) correlation spectra (Fig. 2A). Isotropic backbone and side chain chemical shifts of AFA-PLN were previously reported using solution NMR in DPC micelles [16,24], which allows for a direct comparison between membrane mimicking systems on AFA-PLN's structure. Importantly, the hydrophobic domain II chemical shifts were markedly similar between micelles and bilayers (Fig. 2B and C). Given the sensitivity of backbone chemical shifts to secondary structure, this confirms that the structure of domain II is helical in both DPC micelles and lipid bilayers. The ^{13}C chemical shift index (CSI) $(\delta_{C\alpha} - \delta_{C\beta}) - (\delta_{C\alpha,RC} - \delta_{C\beta,RC})$ [43] of domain Ib in lipid bilayers indicates a greater extent of helicity than we observed in DPC micelles. Based on CSI values, we estimated that ~50% was helical in micelles, based on a helicity of ~100% in lipid bilayers. This has important ramifications for SERCA inhibition, since we have previously shown that the hydrophilic domain Ib of AFA-PLN is in equilibrium between folded (helical) and unfolded states [25,26], which plays a role the ATPase inhibition. This difference may be due to the shorter chain length of the micelles (C12 for DPC) compared to the lipids (~C18 for egg lipids) or the intrinsic curvature and more dynamic nature of the micelles.

3.2. Domain Ia conformation in neutral and negatively charged isotropic bicelles

In analogy to the classic model of amphipathic helix folding [44,45], we recently found that domain Ia of AFA-PLN exists in equilibrium between at least four conformational states [26]. In micelles, these states are in fast exchange on the NMR timescale with the most populated state possessing helical structure with the hydrophobic face inserted into the micelle. In contrast, Baldus and co-workers [46] studied AFA-PLN in DMPC vesicles using MAS solid-state NMR and concluded domain Ia was unfolded and membrane detached based on the random coil chemical shifts.

To probe the structure of domain Ia in lipids we reconstituted [U-^{13}C, ^{15}N] labeled AFA-PLN into isotropic DMPC/DHPC bicelles with a DMPC:DHPC ratio of 1:3 ($q = 0.33$). The [^{1}H, ^{15}N] HSQC spectrum (Fig. 3A) showed only ~40% of the resonances that were observed in DPC micelles. These resonances were assigned using HN(CO)CαA and HNCACBβ solution NMR experiments, and were confirmed to be residues from domain Ia and the loop. This suggested that domain Ia was significantly more dynamic than domain Ib or II, and did not assume the overall rotational correlation time of the bicelle. The failure to observe resonances from transmembrane domains in isotropic bicelles has been documented in other membrane protein systems such as those from the small multidrug resistance family [47].

In Fig. 3B, we plot the ^{13}C CSI $(\delta_{C\alpha} - \delta_{C\beta})$ for full-length AFA-PLN obtained in isotropic bicelles, DPC micelles, and the values obtained from a cytoplasmic domain peptide (PLN_{1-20}) [48]. The chemical shifts in isotropic bicelles are intermediate between shifts in DPC micelles (AFA-PLN_{DPC}, helical and mostly T state) and the shifts for a peptide corresponding to residues 1–20 of PLN [48] (PLN_{1-20}, unfolded and mostly R state). Thus, in isotropic bicelles the conformational equilibrium is shifted to a more unfolded state than in DPC micelles, but still retains helical character. The latter which is in contrast to the previous results in DMPC bilayers.

Domain Ia has four Arg and Lys residues (K3, R9, R13, R14), which gives PLN an overall positive charge at physiological pH values. Therefore, the introduction of a negatively charged lipid could potentially increase the association of domain Ia with the bilayer. To test this hypothesis we replaced 33% of the DMPC with DMPG and measured methyl group chemical shifts, since these are the best reporters of the association of domain Ia with lipids [26]. Fig. 4 shows spectra for V4, L7, A11, and A15 methyl groups obtained in DPC, DMPC/DHPC, and DMPC/DMPG/DHPC, as well as for PLN_{1-20} in aqueous solution. The resonances corresponding to PG-containing bicelles shift toward the AFA-PLN_{DPC} peak, while all peaks are on a linear trajectory spanning from PLN_{1-20} to AFA-PLN_{DPC}. This shows that a) domain Ia is in a fast, apparent two-site exchange between lipid-associated and lipid-dissociated conformations, and b) negatively charged bilayers perturb the conformational equilibrium to favor the membrane-associated conformation. While methyl group chemical shifts are sensitive probes of local environment (i.e., membrane attached or detached), they are less sensitive to secondary structure content. To determine whether the increased affinity of domain Ia for negatively charged lipids was associated with increased helicity, we also measured backbone carbonyl (^{13}C′) chemical shifts in isotropic bicelles using an HNCO experiment and compared CSI values [43] to AFA-PLN_{DPC} (Fig. 4E). The CSI values in the presence of PG clearly showed a small but significant increase in the helicity of domain Ia. Thus, the presence of negatively charged lipids increased the population of the T state, and also support the unfolding/folding conformational model by which domain Ia exchanges between a helical and membrane embedded conformation and one that is unfolded and detached from the surface.

3.3. MAS in DMPC lipids

To validate our results in detergent micelles and isotropic bicelles, we also used MAS experiments with AFA-PLN reconstituted into MLVs. It is well-known that INEPT based transfers filter out immobile domains due to short transverse relaxation times [46]. Using refocused INEPT and CP-based experiments of [U-^{13}C, ^{15}N] AFA-PLN we detected chemical shifts of AFA-PLN at 30 °C in DMPC vesicles that were in excellent agreement with previously published results in the same lipid bilayers and temperature [46]. However, due to the abundance of transmembrane domain residues (~60% of the protein), CP-based spectra were significantly overlapped, which necessitated the use of selectively labeled samples in domain Ia. We synthesized AFA-PLN with Val4, Leu7, Ala11, Ile12, Ala15 and Ile18 [U-^{13}C, ^{15}N] labeled (AFA-PLN_{6cyt}) and acquired 2D DARR spectra at 30 °C. From these experiments we were able to detect intense peaks that corresponded to these six labels. Some of the observed chemical shifts were identical to the random coil values measured from refocused INEPT experiments (Fig. 5). However, we also detected several peaks in the DARR spectrum that were absent from the rINEPT experiment. Specifically, we identified a second population of peaks with ^{13}C chemical shifts consistent with a helical conformation of PLN. In contrast to DPC micelles and isotropic bicelles, the two states observed in the DARR experiments were in slow exchange on the NMR time scale (two peaks are observed in the spectrum).

Table 1
Synthetically labeled AFA-PLN samples.

Sample	[^{13}C, ^{15}N] Residues
1	V4, L7, A11, I12, A15, I18
2	N30, L31, F32, I33
3	N34, F35, A36, L37, I38
4	L39, I40, F41, L42
5	L44, I45, A46, I47
6	A24, I48, V49, L51

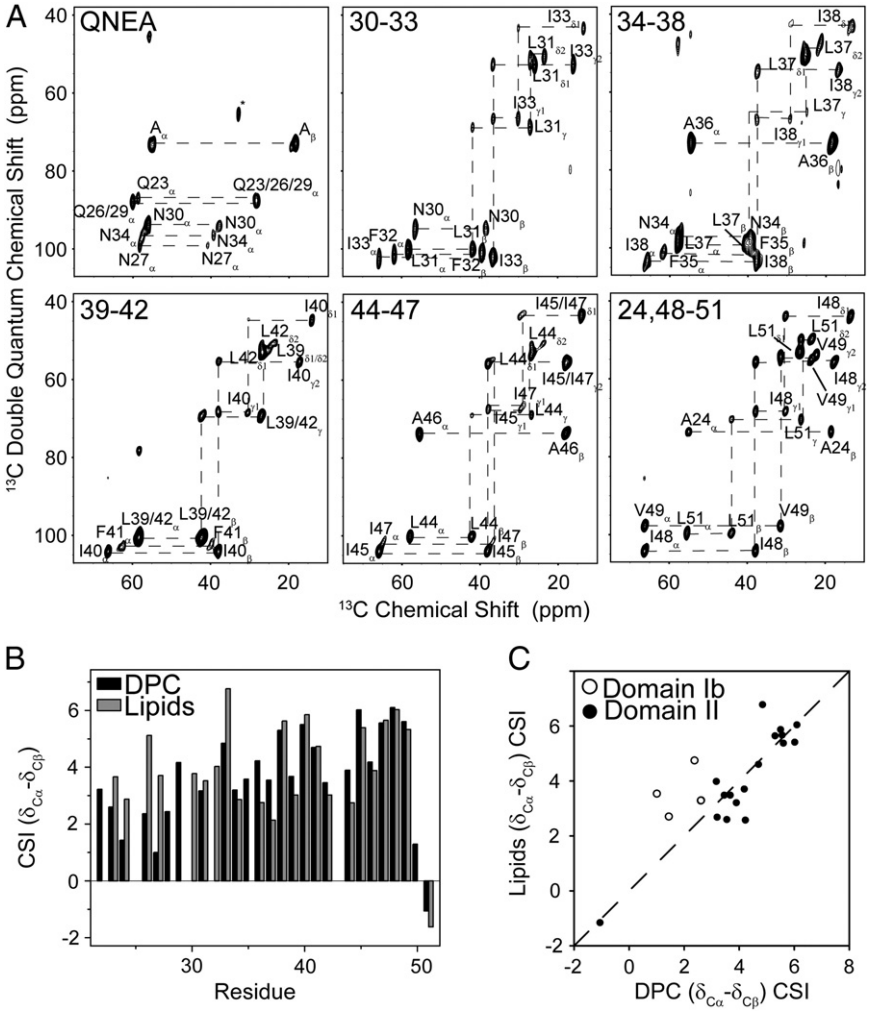

Fig. 2. Assignment of domain Ib and II in lipids and comparison with DPC micelles. A.) SQ-DQ correlation experiments of AFA-PLN reconstituted into egg PC/PE/PA 8/1/1. B.) $^{13}C_\alpha$–$^{13}C_\beta$ CSI for residues in domain Ib and II of AFA-PLN in DPC micelles and egg lipids. CSI was calculated as $\delta_{13C\alpha} - \delta_{13C\beta} - (\delta_{13C\alpha,RC} - \delta_{13C\beta,RC})$, where RC stands for the random coil chemical shifts [43]. C.) Correlation between CSI values in DPC micelles and egg lipids. Residues in domain Ib are shown as open circles and residues in domain II as filled circles.

3.4. Effect of temperature on the conformational equilibria of domain Ia

To determine the effect of temperature on the conformational equilibrium of AFA-PLN we acquired an additional DARR experiment at −25 °C. At this temperature the helical chemical shifts dominated the spectrum showing that the conformational equilibrium has shifted to favor the T state. With the exception of Ala15 at the C-terminal end of the domain Ia helix, there is excellent agreement between the T state chemical shifts and the shifts of AFA-PLN$_{DPC}$ (Fig. 6). This shows that the domain Ia helix (T state) may be slightly shorter in lipid bilayers than in DPC micelles. Importantly, this also implies that AFA-PLN samples similar conformational space regardless of the membrane mimicking system (detergent micelle, isotropic bicelle, lipid bilayer, etc.), but that the populations of the conformational states are very sensitive to the choice of membrane mimic.

Solution NMR data in DPC micelles show at least four resolved conformational states (T, T′, R, and R′). However, it is possible that the T′ and R′ states have chemical shifts very similar to the T and R states and, therefore, are indistinguishable in the MAS spectra (i.e., broader lines than the detergent micelle spectra). Alternatively, the T′ and R′ states may be scarcely populated in lipids and therefore not detectable.

3.5. MAS in native SR lipids

While DMPC vesicles are a well-characterized model membrane system, they lack several characteristics of a native lipid bilayer of the SR. For example, the SR membrane, where PLN is embedded, contains a significant portion of PE and PS head groups and has an average lipid chain length of 18 carbons compared to the 14 carbons of DMPC [32]. To support our conclusions in synthetic lipid membranes, we reconstituted AFA-PLN$_{6cyt}$ into lipids extracted from the SR of rabbit skeletal muscle. In these lipids, DARR spectra acquired at −25 °C and 20 °C were in good agreement with spectra obtained using DMPC lipids (Fig. 7). Spectra acquired at −25 °C and 20 °C show multiple peaks with a shift in equilibrium toward the T state component at the lower temperature. Taken together, these data confirmed that the conformational equilibrium of AFA-PLN is also present in native lipids.

3.6. Solvent accessibility of T and R states

To further support our assignment of two populations (T and R states), we used paramagnetic relaxation enhancement (PRE) and acquired DARR experiments in SR lipids in the presence and absence of 20 mM water-soluble Gd^{3+}. These experiments were performed at 4 °C to have approximately equal intensities of R and T state peaks. Fig. 8 shows that the R state (36% signal retained on average) is quenched more than the T state (63% signal retained on average) for residues Val4, Leu7, Ala11, and Ile12. Ala15 and Ile18 were excluded from the analysis since they have similar chemical shifts in the T and R states. These results confirmed that the T state is membrane-associated and solvent-protected, while the R state is exposed to

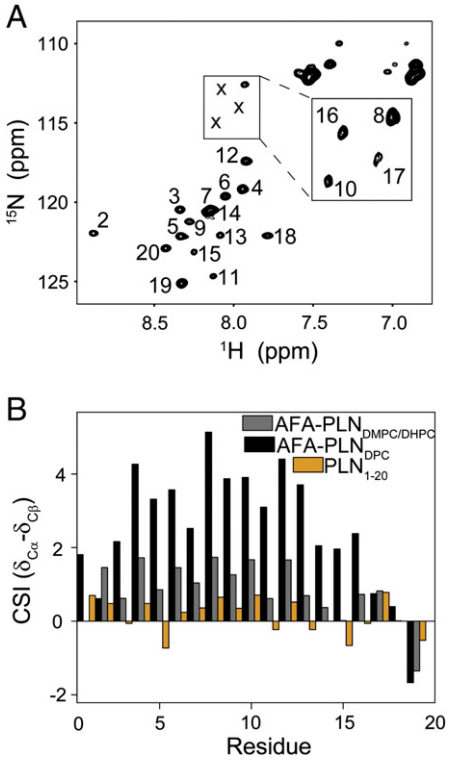

Fig. 3. PLN in isotropic bicelles. A.) [^{15}N]-HSQC of AFA-PLN in DMPC/DHPC isotropic bicelles with q = 0.33. Peaks corresponding to residues S10, S16 and T17 (marked with x) were detected at a lower noise level as shown in the inset. B.) Helicity of domain Ia in different membrane mimics. $^{13}C_\alpha$–$^{13}C_\beta$ CSI for domain Ia of AFA-PLN in DPC micelles (black), DMPC/DHPC isotropic bicelles (red) and a peptide corresponding to residues 1–20 of PLN [48] (PLN$_{1-20}$, orange).

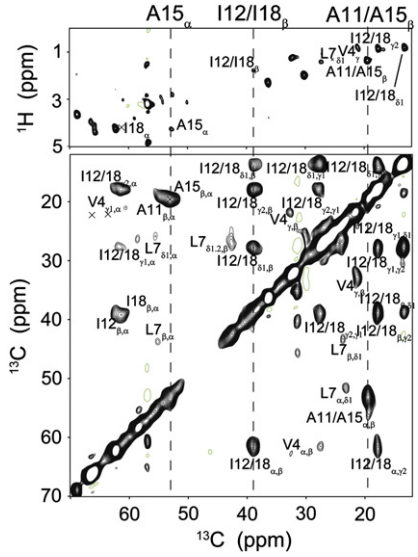

Fig. 5. CP-transfers detect resonances that are absent from INEPT-based experiments. Comparison of rINEPT (top) and DARR (bottom, 200 ms mixing time) experiments of AFA-PLN$_{6cyt}$ reconstituted into d_{54}-DMPC MLVs at 30 °C. Dashed lines highlight examples of peaks that are detected in both experiments.

solvent, and are thus in strong agreement with our conformational model of AFA-PLN [26].

4. Discussion

The secondary structure content of the transmembrane domain II of PLN is preserved in all membrane mimicking systems, spanning from organic solvents [49] and detergent micelles [24] to lipid bilayers of different compositions [15,16]. In particular, the chemical shifts obtained in DPC micelles and lipid bilayers are in remarkable agreement (Fig. 2). This suggests that while detergent micelles have limitations, they can still offer structural insights on rigid, membrane-spanning portions of membrane proteins. On the other hand, DPC micelles altered the conformational equilibria for domains Ia and Ib of AFA-PLN that are more malleable and solvent exposed [21,50]. For instance, the chemical shifts for domain Ib in lipids have a greater extent of helicity than those obtained in DPC micelles, although in both membrane mimics the predominant conformation is helical. In contrast, the amphipathic domain Ia is significantly more helical in DPC micelles than in lipids, revealing an almost complete shift towards the T state in this detergent. The latter is in agreement with the topology of AFA-PLN determined in mechanically aligned DOPC/DOPE bilayers [16]. Interestingly, in lipid vesicles and native SR lipids, the R and T states exchange on a slow time scale. Thus, the dynamic nature of the detergent and the isotropic bicelle may act to lower the activation energy barrier between these conformational states, which would alter the exchange rates. The multiple

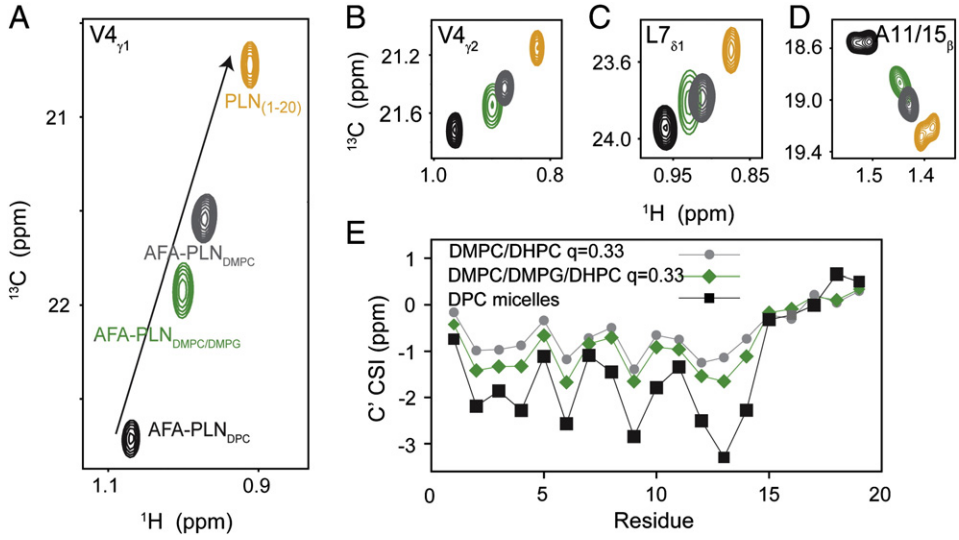

Fig. 4. Negatively charged lipids shifts the equilibrium towards the T state. A–D.) ^{13}C HSQC experiments of AFA-PLN in DPC micelles (black, T state), DMPC/DHPC, q = 0.33, isotropic bicelles (gray) DMPC/DMPG/DHPC (4:1 DMPC:DMPG) isotropic bicelles (green) and PLN$_{1-20}$ (orange, R state). E.) CO CSI for AFA-PLN in different membrane mimics.

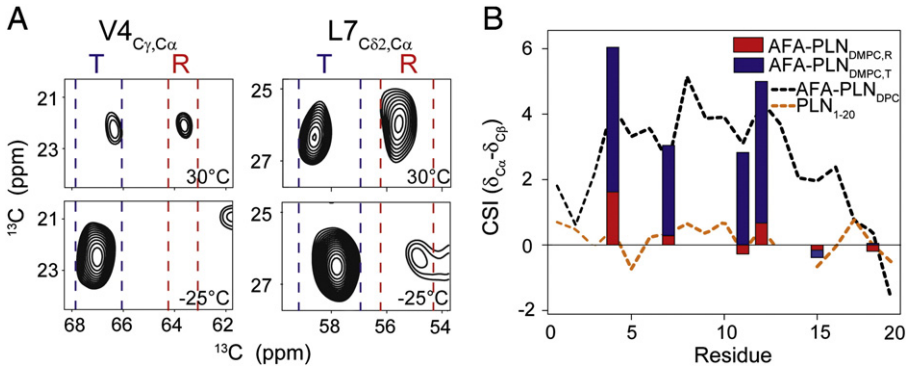

Fig. 6. Conformational equilibrium of AFA-PLN in DMPC at different temperatures. A.) Cross-peaks from DARR spectra corresponding to a C_α–C_γ correlation for Val4 (left) and C_α–$C_{\delta 2}$ correlation for Leu7 (right) at 30 °C (top) and −25 °C (bottom). Blue and red dashed lines highlight the chemical shift regions of the folded T state and unfolded R state respectively. B.) Cα–Cβ CSI of the folded T state (measured from experiments at −25 °C, blue bars) and unfolded R state (measured from experiments at 30 °C, red bars) compared to DPC micelles (black dotted lines, predominantly T state) and PLN_{1-20} (orange dotted line, predominantly R state).

populations observed in lipids allowed us to analyze the chemical shifts and exposure to water separately. Our PRE measurements show that the R state is unfolded and solvent-exposed, as proposed previously [26]. Also, the excellent overlay between spectra acquired in SR lipids and DMPC suggests that the conformations of AFA-PLN are conserved between the different lipid systems.

It is important to stress that neither the unfolded R state nor the folded T state is analogous to the architecture of the pentameric PLN solved in DPC micelles with domain Ia in a helical, membrane-dissociated conformation [51]. However, our data help explain the results reported by Baldus and co-workers [46] from MAS experiments in DMPC lipid vesicles. Using INEPT-based transfer experiments, the flexible R state of AFA-PLN was detected, filtering out the resonances of the T state. We showed that by using both CP- and INEPT-based transfers it is possible to detect both conformational states of AFA-PLN (T and R states). It is possible that Baldus and co-workers did not observe the T state of domain Ia because of the the low lipid/protein ratio, which promotes the R state, since a smaller amount of lipid surface area would be present. In addition to observing both T and R states, we also found that the AFA-PLN conformational equilibrium has strong temperature dependence, with the T state favored at lower temperature and the R state at higher temperature. This behavior is similar to that observed for the membrane-active peptide Tat, which is in a random coil conformation at high temperature but forms a β-sheet at lower temperatures [52]. The dependence of AFA-PLN domain Ia on temperature as well as the choice of membrane mimic shows that caution must be taken when comparing experiments acquired at different temperatures and in different membrane-environments.

At temperatures above 20 °C the R state dominates over the T state (Fig. 6). In this regard domain Ia of PLN resembles an intrinsically disordered protein, which folds into a helix upon interaction with the lipid bilayer [53,54]. In addition to the bilayer interactions, PLN binds a number of different proteins. We have recently shown that protein kinase A (PKA) preferentially binds an extended conformation of domain Ia [48,55]. Thus, the malleability of PLN allows for recognition by different binding partners. Further research is needed to determine what conformation(s) of PLN is (are) recognized by other proteins. Nevertheless, since promotion of the R state relieves the inhibitory effect of SERCA by PLN, perturbations that alter the T/R equilibrium directly affect the regulation of SERCA. One example of this is the introduction of negatively charged PG lipids, which promotes the T state conformation (Fig. 4). This observation suggests that lipid–PLN interactions may regulate SERCA function.

In our first characterization of the calcium regulatory cycle, we defined PLN as an allosteric modulator of SERCA, without specifying its role in the *allosteric* phenomenon [19,28,29,56]. In light of our

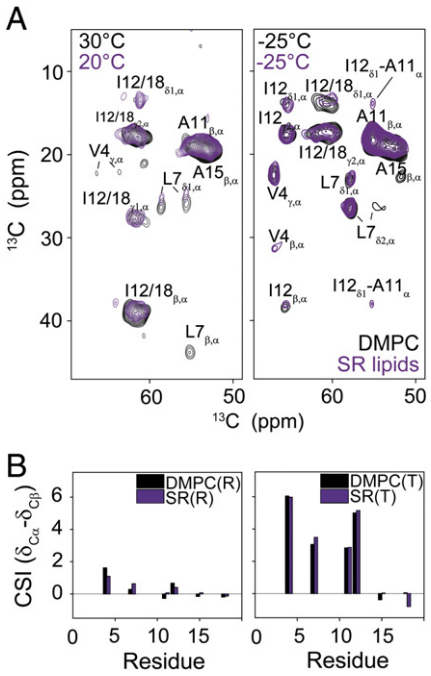

Fig. 7. The conformational equilibrium of AFA-PLN is conserved in native SR lipids. A.) Overlay of DARR experiments of $AFA\text{-}PLN_{6cyt}$ reconstituted into DMPC (black) or extracted SR lipids (purple). Experiments in SR lipids were acquired at −25 °C and 20 °C and experiments in DMPC were acquired at −25 °C and 30 °C. All experiments utilized a 200 ms mixing time. B.) $^{13}C_\alpha$–$^{13}C_\beta$ CSI of the R and T state components in DMPC (black) and SR lipids (purple).

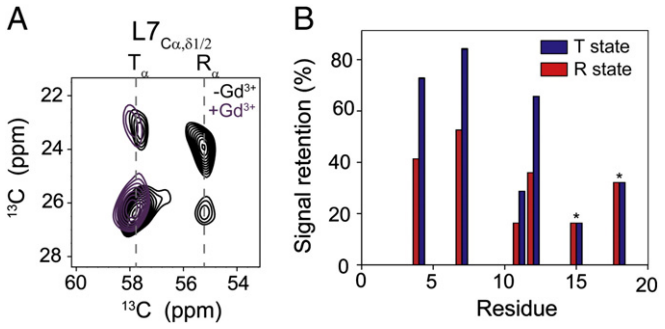

Fig. 8. The T state is inserted into the lipid bilayer. A.) Region from DARR spectra of $AFA\text{-}PLN_{6cyt}$ in SR lipids acquired in the presence (turquoise) and absence (black) of 20 mM Gd^{3+}. B.) Signal retention of peaks corresponding to the T and R states quantified from DARR spectra acquired in the presence and absence of 20 mM Gd^{3+}. Signal retention was calculated as I_{Gd3+}/I_0 in DARR spectra quenching of T and R states of AFA-PLN. For Ala15 and Ile18 the T and R state peaks are overlapped and therefore the signal retention reports on a combination of T and R states.

recent results, we propose that the allosteric regulation of SERCA by PLN includes intramembrane, long-range interactions [57–60], where PLN controls Ca^{2+} transport, preceded by a selection of active conformations of PLN by SERCA from a pre-existing conformational equilibrium [59–63] (Fig. 1). These phenomena are interconnected and constitute part of the complex mechanism for allosteric signal transduction in the heart muscle. Based on the data presented here, it is becoming clear that by fine-tuning PLN conformational equilibria, lipid membranes represent a third element for allosteric control of SERCA. Through the alteration of the lipid composition from diet or pathophysiology [64–66], it is possible that lipid membranes *shape* both the conformation and function of the SERCA/PLN complex, affecting muscle contractility.

From a more biophysical point of view, these studies revive an old concept of the allosteric regulation of lipid membranes [1]. Furthermore, the possibility of using solid-state NMR to study membrane proteins under native lipid compositions allows for the characterization of lipid–protein interactions at the atomic level to reveal the role of lipids in activation and deactivation of protein function.

Acknowledgements

We thank Dan Mullen for synthesis of AFA-PLN protein, Rahel Woldeyes for testing AFA-PLN activity. This work was supported by the National Institute of Health (GM64742 to G.V.) and a pre-doctoral fellowship to M.G. from the American Heart Association (10PRE3860050).

References

[1] R.N. Farias, B. Bloj, R.D. Morero, F. Sineriz, R.E. Trucco, Regulation of allosteric membrane-bound enzymes through changes in membrane lipid compostition, Biochim. Biophys. Acta 415 (1975) 231–251.
[2] A. McDermott, T. Polenova, Solid state NMR: new tools for insight into enzyme function, Curr. Opin. Struct. Biol. 17 (2007) 617–622.
[3] V. Lange, J. Becker-Baldus, B. Kunert, B.J. van Rossum, F. Casagrande, A. Engel, Y. Roske, F.M. Scheffel, E. Schneider, H. Oschkinat, A MAS NMR study of the bacterial ABC transporter ArtMP, ChemBioChem 11 (2010) 547–555.
[4] M. Tang, L.J. Sperling, D.A. Berthold, A.E. Nesbitt, R.B. Gennis, C.M. Rienstra, Solid-state NMR study of the charge-transfer complex between ubiquinone-8 and disulfide bond generating membrane protein DsbB, J. Am. Chem. Soc. 133 (2011) 4359–4366.
[5] S.D. Cady, K. Schmidt-Rohr, J. Wang, C.S. Soto, W.F. Degrado, M. Hong, Structure of the amantadine binding site of influenza M2 proton channels in lipid bilayers, Nature 463 (2010) 689–692.
[6] L. Shi, I. Kawamura, K.H. Jung, L.S. Brown, V. Ladizhansky, Conformation of a seven-helical transmembrane photosensor in the lipid environment, Angew. Chem. Int. Ed. Engl. 50 (2011) 1302–1305.
[7] F.D. Mills, V.C. Antharam, O.K. Ganesh, D.W. Elliott, S.A. McNeill, J.R. Long, The helical structure of surfactant peptide KL4 when bound to POPC: POPG lipid vesicles, Biochemistry 47 (2008) 8292–8300.
[8] R. Linser, M. Dasari, M. Hiller, V. Higman, U. Fink, J.M. Lopez Del Amo, S. Markovic, L. Handel, B. Kessler, P. Schmieder, D. Oesterhelt, H. Oschkinat, B. Reif, Proton-detected solid-state NMR spectroscopy of fibrillar and membrane proteins, Angew. Chem. Int. Ed. Engl. 50 (2011) 4508–4512.
[9] W. Qiang, Y. Sun, D.P. Weliky, A strong correlation between fusogenicity and membrane insertion depth of the HIV fusion peptide, Proc. Natl. Acad. Sci. U. S. A. 106 (2009) 15314–15319.
[10] H. Saito, A. Naito, NMR studies on fully hydrated membrane proteins, with emphasis on bacteriorhodopsin as a typical and prototype membrane protein, Biochim. Biophys. Acta 1768 (2007) 3145–3161.
[11] V.S. Bajaj, M.L. Mak-Jurkauskas, M. Belenky, J. Herzfeld, R.G. Griffin, Functional and shunt states of bacteriorhodopsin resolved by 250 GHz dynamic nuclear polarization-enhanced solid-state NMR, Proc. Natl. Acad. Sci. U. S. A. 106 (2009) 9244–9249.
[12] M.R. de Planque, D.T. Rijkers, J.I. Fletcher, R.M. Liskamp, F. Separovic, The alphaM1 segment of the nicotinic acetylcholine receptor exhibits conformational flexibility in a membrane environment, Biochim. Biophys. Acta 1665 (2004) 40–47.
[13] A.A. De Angelis, D.H. Jones, C.V. Grant, S.H. Park, M.F. Mesleh, S.J. Opella, NMR experiments on aligned samples of membrane proteins, Methods Enzymol. 394 (2005) 350–382.
[14] M. Sharma, M. Yi, H. Dong, H. Qin, E. Peterson, D.D. Busath, H.X. Zhou, T.A. Cross, Insight into the mechanism of the influenza A proton channel from a structure in a lipid bilayer, Science 330 (2010) 509–512.
[15] R. Verardi, L. Shi, N.J. Traaseth, N. Walsh, G. Veglia, Structural topology of phospholamban pentamer in lipid bilayers by a hybrid solution and solid-state NMR method, Proc. Natl. Acad. Sci. U. S. A. 108 (2011) 9101–9106.
[16] N.J. Traaseth, L. Shi, R. Verardi, D.G. Mullen, G. Barany, G. Veglia, Structure and topology of monomeric phospholamban in lipid membranes determined by a hybrid solution and solid-state NMR approach, Proc. Natl. Acad. Sci. U. S. A. 106 (2009) 10165–10170.
[17] J.J. Buffy, N.J. Traaseth, A. Mascioni, P.L. Gor'kov, E.Y. Chekmenev, W.W. Brey, G. Veglia, Two-dimensional solid-state NMR reveals two topologies of sarcolipin in oriented lipid bilayers, Biochemistry 45 (2006) 10939–10946.
[18] N.J. Traaseth, J.J. Buffy, J. Zamoon, G. Veglia, Structural dynamics and topology of phospholamban in oriented lipid bilayers using multidimensional solid-state NMR, Biochemistry 45 (2006) 13827–13834.
[19] N.J. Traaseth, K.N. Ha, R. Verardi, L. Shi, J.J. Buffy, L.R. Masterson, G. Veglia, Structural and dynamic basis of phospholamban and sarcolipin inhibition of $Ca^{(2+)}$-ATPase, Biochemistry 47 (2008) 3–13.
[20] D.H. MacLennan, E.G. Kranias, Phospholamban: a crucial regulator of cardiac contractility, Nat. Rev. Mol. Cell Biol. 4 (2003) 566–577.
[21] E.E. Metcalfe, J. Zamoon, D.D. Thomas, G. Veglia, (1)H/(15)N heteronuclear NMR spectroscopy shows four dynamic domains for phospholamban reconstituted in dodecylphosphocholine micelles, Biophys. J. 87 (2004) 1205–1214.
[22] C.B. Karim, T.L. Kirby, Z. Zhang, Y. Nesmelov, D.D. Thomas, Phospholamban structural dynamics in lipid bilayers probed by a spin label rigidly coupled to the peptide backbone, Proc. Natl. Acad. Sci. U. S. A. 101 (2004) 14437–14442.
[23] S. Abu-Baker, J.X. Lu, S. Chu, C.C. Brinn, C.A. Makaroff, G.A. Lorigan, Side chain and backbone dynamics of phospholamban in phospholipid bilayers utilizing (2)h and (15)n solid-state NMR spectroscopy, Biochemistry 46 (2007) 11695–11706.
[24] J. Zamoon, A. Mascioni, D.D. Thomas, G. Veglia, NMR solution structure and topological orientation of monomeric phospholamban in dodecylphosphocholine micelles, Biophys. J. 85 (2003) 2589–2598.
[25] N.J. Traaseth, G. Veglia, Probing excited states and activation energy for the integral membrane protein phospholamban by NMR CPMG relaxation dispersion experiments, Biochim. Biophys. Acta 1798 (2010) 77–81.
[26] M. Gustavsson, N.J. Traaseth, C.B. Karim, E.L. Lockamy, D.D. Thomas, G. Veglia, Lipid-mediated folding/unfolding of phospholamban as a regulatory mechanism for the sarcoplasmic reticulum $Ca^{(2+)}$-ATPase, J. Mol. Biol. 408 (2011) 755–765.
[27] C.B. Karim, Z. Zhang, E.C. Howard, K.D. Torgersen, D.D. Thomas, Phosphorylation-dependent conformational switch in spin-labeled phospholamban bound to SERCA, J. Mol. Biol. 358 (2006) 1032–1040.
[28] J. Zamoon, F. Nitu, C. Karim, D.D. Thomas, G. Veglia, Mapping the interaction surface of a membrane protein: unveiling the conformational switch of phospholamban in calcium pump regulation, Proc. Natl. Acad. Sci. U. S. A. 102 (2005) 4747–4752.
[29] K.N. Ha, N.J. Traaseth, R. Verardi, J. Zamoon, A. Cembran, C.B. Karim, D.D. Thomas, G. Veglia, Controlling the inhibition of the sarcoplasmic Ca^{2+} −ATPase by tuning phospholamban structural dynamics, J. Biol. Chem. 282 (2007) 37205–37214.
[30] D.M. Kaye, M. Hoshijima, K.R. Chien, Reversing advanced heart failure by targeting Ca^{2+} cycling, Annu. Rev. Med. 59 (2008) 13–28.
[31] F. del Monte, S.E. Harding, G.W. Dec, J.K. Gwathmey, R.J. Hajjar, Targeting phospholamban by gene transfer in human heart failure, Circulation 105 (2002) 904–907.
[32] R.J. Bick, L.M. Buja, W.B. Van Winkle, G.E. Taffet, Membrane asymmetry in isolated canine cardiac sarcoplasmic reticulum: comparison with skeletal muscle sarcoplasmic reticulum, J. Membr. Biol. 164 (1998) 169–175.
[33] C.B. Karim, C.G. Marquardt, J.D. Stamm, G. Barany, D.D. Thomas, Synthetic null-cysteine phospholamban analogue and the corresponding transmembrane domain inhibit the Ca-ATPase, Biochemistry 39 (2000) 10892–10897.
[34] B. Buck, J. Zamoon, T.L. Kirby, T.M. DeSilva, C. Karim, D. Thomas, G. Veglia, Overexpression, purification, and characterization of recombinant Ca-ATPase regulators for high-resolution solution and solid-state NMR studies, Protein Expr. Purif. 30 (2003) 253–261.
[35] K.I. Tong, M. Yamamoto, T. Tanaka, A simple method for amino acid selective isotope labeling of recombinant proteins in *E. coli*, J. Biomol. NMR 42 (2008) 59–67.
[36] L.G. Reddy, R.L. Cornea, D.L. Winters, E. McKenna, D.D. Thomas, Defining the molecular components of calcium transport regulation in a reconstituted membrane system, Biochemistry 42 (2003) 4585–4592.
[37] K. Takegoshi, S. Nakamura, T. Terao, $^{13}C-^{1}H$ dipolar-assisted rotational resonance in magic-angle spinning NMR, Chem. Phys. Lett. 344 (2001) 631.
[38] G.A. Morris, R.J. Freeman, Enhancement of nuclear magnetic resonance signals by polarization transfer, J. Am. Chem. Soc. 101 (1979) 760–762.
[39] A.E. Bennett, C.M. Rienstra, M. Auger, K.V. Lakshmi, R.G. Griffin, Heteronuclear decoupling in rotating solids, J. Chem. Phys. 103 (1995) 6951–6958.
[40] M. Hohwy, C.M. Rienstra, C.P. Jaroniec, R.G. Griffin, Fivefold symmetric homonuclear dipolar recoupling in rotating solids: application to double quantum spectroscopy, J. Chem. Phys. 110 (1999) 7983–7992.
[41] F. Delaglio, S. Grzesiek, G.W. Vuister, G. Zhu, J. Pfeifer, A. Bax, NMRPipe: a multidimensional spectral processing system based on UNIX pipes, J. Biomol. NMR 6 (1995) 277–293.
[42] T.D. Goddard, D.G. Kneller, SPARKY 3 (1999), University of California, San Francisco.
[43] H. Zhang, S. Neal, D.S. Wishart, RefDB: a database of uniformly referenced protein chemical shifts, J. Biomol. NMR 25 (2003) 173–195.
[44] S.H. White, W.C. Wimley, Membrane protein folding and stability: physical principles, Annu. Rev. Biophys. Biomol. Struct. 28 (1999) 319–365.
[45] D.M. Engelman, Y. Chen, C.N. Chin, A.R. Curran, A.M. Dixon, A.D. Dupuy, A.S. Lee, U. Lehnert, E.E. Matthews, Y.K. Reshetnyak, A. Senes, J.L. Popot, Membrane protein folding: beyond the two stage model, FEBS Lett. 555 (2003) 122–125.
[46] O.C. Andronesi, S. Becker, K. Seidel, H. Heise, H.S. Young, M. Baldus, Determination of membrane protein structure and dynamics by magic-angle-spinning solid-state NMR spectroscopy, J. Am. Chem. Soc. 127 (2005) 12965–12974.

[47] S.F. Poget, S.M. Cahill, M.E. Girvin, Isotropic bicelles stabilize the functional form of a small multidrug-resistance pump for NMR structural studies, J. Am. Chem. Soc. 129 (2007) 2432–2433.
[48] L.R. Masterson, T. Yu, L. Shi, Y. Wang, M. Gustavsson, M.M. Mueller, G. Veglia, cAMP-Dependent Protein Kinase A Selects the Excited State of the Membrane Substrate Phospholamban, J. Mol. Biol. 412 (2011) 155–164.
[49] S. Lamberth, H. Schmid, M. Muenchbach, T. Vorherr, J. Krebs, E. Carafoli, C. Griesinger, NMR solution structure of phospholamban, Helv. Chim. Acta 83 (2000) 2141–2151.
[50] N.J. Traaseth, G. Veglia, Probing excited states and activation energy for the integral membrane protein phospholamban by NMR CPMG relaxation dispersion experiments, Biochim. Biophys. Acta 1798 (2010) 77–81.
[51] K. Oxenoid, J.J. Chou, The structure of phospholamban pentamer reveals a channel-like architecture in membranes, Proc. Natl. Acad. Sci. U. S. A. 102 (2005) 10870–10875.
[52] Y. Su, A.J. Waring, P. Ruchala, M. Hong, Membrane-bound dynamic structure of an arginine-rich cell-penetrating peptide, the protein transduction domain of HIV TAT, from solid-state NMR, Biochemistry 49 (2010) 6009–6020.
[53] T. Mittag, L.E. Kay, J.D. Forman-Kay, Protein dynamics and conformational disorder in molecular recognition, J. Mol. Recognit. 23 (2010) 105–116.
[54] P.E. Wright, H.J. Dyson, Linking folding and binding, Curr. Opin. Struct. Biol. 19 (2009) 31–38.
[55] L.R. Masterson, C. Cheng, T. Yu, M. Tonelli, A.P. Kornev, S.S. Taylor, G. Veglia, Dynamics connect substrate recognition to catalysis in protein kinase A, Nat. Chem. Biol. 6 (2010) 821–828.
[56] N.J. Traaseth, D.D. Thomas, G. Veglia, Effects of Ser16 phosphorylation on the allosteric transitions of phospholamban/Ca($^{2+}$)-ATPase complex, J. Mol. Biol. 358 (2006) 1041–1050.
[57] J. Monod, J. Wyman, J.P. Changeux, On the nature of allosteric transitions: a plausible model, J. Mol. Biol. 12 (1965) 88–118.
[58] D.E. Koshland Jr., G. Nemethy, D. Filmer, Comparison of experimental binding data and theoretical models in proteins containing subunits, Biochemistry 5 (1966) 365–385.
[59] C.J. Tsai, A. Del Sol, R. Nussinov, Protein allostery, signal transmission and dynamics: a classification scheme of allosteric mechanisms, Mol. Biosyst. 5 (2009) 207–216.
[60] Q. Cui, M. Karplus, Allostery and cooperativity revisited, Protein Sci. 17 (2008) 1295–1307.
[61] R.G. Smock, L.M. Gierasch, Sending signals dynamically, Science 324 (2009) 198–203.
[62] B. Ma, R. Nussinov, Enzyme dynamics point to stepwise conformational selection in catalysis, Curr. Opin. Chem. Biol. 14 (2010) 652–659.
[63] S.R. Tzeng, C.G. Kalodimos, Dynamic activation of an allosteric regulatory protein, Nature 462 (2009) 368–372.
[64] G.E. Taffet, T.T. Pham, D.L. Bick, M.L. Entman, H.J. Pownall, R.J. Bick, The calcium uptake of the rat heart sarcoplasmic reticulum is altered by dietary lipid, J. Membr. Biol. 131 (1993) 35–42.
[65] R.E. Mrak, S. Fleischer, Lipid composition of sarcoplasmic reticulum from mice with muscular dystrophy, Muscle Nerve 5 (1982) 439–446.
[66] A.G. Krainev, D.A. Ferrington, T.D. Williams, T.C. Squier, D.J. Bigelow, Adaptive changes in lipid composition of skeletal sarcoplasmic reticulum membranes associated with aging, Biochim. Biophys. Acta 1235 (1995) 406–418.